# Six-Transmembrane Epithelial Antigen of Prostate 3 Promotes Hepatic Insulin Resistance and Steatosis

**Ting Ding**[1,‡], **Siping Chen**[1,‡], **Wenchang Xiao**[2,3,‡] , **Zhen Liu**[4], **Jun Tu**[3], **Yongjie Yu**[3], **Bizhen Dong**[3], **Wenping Chen**[1*], and **Yong Zeng**[5*]

[1]Department of Endocrinology, and [2]Department of Cardiovascular Surgery, Huanggang Central Hospital, Huanggang, China; [3]Huanggang Institute of Translational Medicine, Huanggang Central Hospital, Huanggang, China; [4]Department of Cardiology, Renmin Hospital of Wuhan University, Wuhan, China; [5]Department of Stomatology, Huanggang Central Hospital, Huanggang, China

**Abstract** Nonalcoholic fatty liver disease (NAFLD) is a clinicopathological syndrome characterized by excessive deposition of fatty acids in the liver. Further deterioration leads to nonalcoholic steatohepatitis, cirrhosis, and hepatocellular carcinoma, creating a heavy burden on human health and the social economy. Currently, there are no effective and specific drugs for the treatment of NAFLD. Therefore, it is important to further investigate the pathogenesis of NAFLD and explore effective therapeutic targets for the prevention and treatment of the disease. Six-transmembrane epithelial antigen of prostate 3 (STEAP3), a STEAP family protein, is a metalloreductase. Studies have shown that it can participate in the regulation of liver ischemia-reperfusion injury, hepatocellular carcinoma, myocardial hypertrophy, and other diseases. In this study, we found that the expression of STEAP3 is upregulated in NAFLD. Deletion of STEAP3 inhibits the development of NAFLD in vivo and in vitro, whereas its overexpression promotes palmitic acid/oleic acid stimulation-induced lipid deposition in hepatocytes. Mechanistically, it interacts with transforming growth factor beta-activated kinase 1 (TAK1) to regulate the progression of NAFLD by promoting TAK1 phosphorylation and activating the TAK1-c-Jun N-terminal kinase/p38 signaling pathway. 🔓 Taken together, our results provide further insight into the involvement of STEAP3 in liver pathology.

**Supplementary key words** STEAP3 • metalloreductase • NAFLD • glucose metabolism disorder • lipid deposition • hepatic steatosis • hepatocytes • PA/OA • TAK1 • JNK/p38 signaling pathway

Nonalcoholic fatty liver disease (NAFLD) is the most prominent cause of chronic liver disease worldwide (1). The many associated hepatic and extrahepatic comorbidities result in a serious public health burden of NAFLD, which is estimated to affect approximately 25% of the world's adult population (2). Continuous lipid accumulation and inflammation are considered basic characteristics of NAFLD progression from simple steatosis to nonalcoholic steatohepatitis (3), which may eventually lead to liver cirrhosis and hepatocellular carcinoma (HCC) (4). Because of sharply increasing morbidity, the discovery of treatments and drugs for these diseases is urgently required (5). In recent years, various molecular targets, which are involved in NAFLD pathogenesis, have been identified (6). However, effective pharmacological therapies for NAFLD are still lacking (7, 8).

The six-transmembrane epithelial antigen of prostate (STEAP) family proteins, consisting of four multitransmembrane proteins, have been reported to affect metal homeostasis via the reduction and uptake of iron and copper (9). Among these proteins, STEAP3 is the major endosomal ferrireductase that participates in various biological processes, including molecular trafficking, cell proliferation, apoptosis, and inflammation (10–12). STEAP3 null mice show microcytic anemia caused by abnormal erythroid maturation, which is thought to be the result of ablation of the ferrireductase of STEAP3 (13). Exosome secretion is also severely compromised in STEAP3-deficient mice via the p53-dependent secretory pathway (14). p53-induced STEAP3 promotes apoptosis and negatively regulates $G_2/M$ transition (12). Moreover, STEAP3 deficiency is responsible for the impaired Toll-like receptor 4-mediated inflammatory response in macrophages (11). In addition, STEAP3 acts as a regulator of inflammation and apoptosis in liver ischemia-reperfusion injury (15). However, the functions of STEAP3 in NAFLD remain poorly understood.

In the current study, we identified a significant increase of STEAP3 expression in the liver of NAFLD

‡These authors contributed equally to this work.
*For correspondence: Wenping Chen, chenwenping@hgyy.org.cn; Yong Zeng, zengyong@hgyy.org.cn.

mice and hepatocytes of a cell model. The deficiency of STEAP3 relieves glucose metabolic disorders and hepatic steatosis in high-fat diet (HFD)-induced mice and palmitic acid/oleic acid (PA/OA)-stimulated primary hepatocytes. In contrast, hepatocytes overexpressing STEAP3 exhibited enhanced lipid accumulation and upregulated gene expression for lipid metabolism. Systematic investigation revealed that inhibition of the MAPK cascade is strongly associated with the deletion of STEAP3 in fatty liver. Furthermore, STEAP3 interacts with transforming growth factor beta-activated kinase 1 (TAK1), a pivotal member of the MAPK signaling pathway in hepatocytes. In addition, inhibition of TAK1 rescued the NAFLD phenotypes induced by STEAP3 overexpression. Collectively, our results indicate that the absence of STEAP3 inhibits the progression of NAFLD by physically interacting with TAK1 and activating the MAPK signaling cascade.

## MATERIALS AND METHODS

### Animals

Eight-week male mice of 20–26 g were included in this study. All mice used for the experiment were housed in a specific pathogen-free animal laboratory with a controlled environment that included temperature ($24 \pm 2°C$), humidity (40–70%), and a 12 h light-dark cycle. The NAFLD model was established by feeding mice an HFD for 24 weeks (HFD containing 20% protein, 60% fat, and 20% carbohydrate; H10060; Huafukang, Beijing, China). Mice in the control group were fed normal chow (NC) diet (catalog no.: 1010086; Xietong Biology, Jiangsu, China). Water was available ad libitum for all mice in all the experiments. All animal protocols were approved by the Animal Care and Use Committee of the Renmin Hospital of Wuhan University. STEAP3-KO mice were purchased from the Texas A&M Institute for Genomic Medicine (mutant cell line: IST13594Cll; TIGM, Germany).

### Detection of physiological parameters

The weight and blood glucose levels of the mice were measured after fasting for 6 h every 4 weeks. Blood insulin levels were estimated using an enzyme-linked immunosorbent assay kit (Cloud-Corp, Wuhan, China). Homeostatic model assessment of insulin resistance was evaluated using the following formula: (fasting blood glucose [mmol/l] × fasting serum insulin [mIU/l])/22.5. Glucose tolerance test assays were performed at the 23rd week as described previously: animals were injected (ip) at a dose of 1 g/kg after 6 h of fasting. Blood glucose levels were measured at baseline and at 15, 30, 60, and 120 min after glucose injection, and the area under the curve was calculated using the conventional trapezoid rule.

Levels of serum lipid triglyceride, total cholesterol, alanine aminotransferase, and aspartate aminotransferase were measured using an ADVIA 2400 Chemistry System Analyzer (Siemens, Tarrytown, NY).

### Histological analysis

Liver sections cut from formaldehyde-fixed and paraffin-embedded liver tissues of experimental mice in a thickness of 5 μm were used for H&E staining (hematoxylin, catalog no.: G1004, Servicebio Co, Ltd, Wuhan, China; eosin, catalog no.: BA-4024, Baso Co, Ltd, Zhuhai, China) to evaluate the morphological change of liver tissue and lipid accumulation, and periodic acid-Schiff staining (periodic acid, catalog no.: BA-4044B; Schiff reagent, catalog no.: BA-4044A, Baso, Zhuhai, China) to evaluate the accumulation of glycogen. Frozen liver sections cut from liver tissues embedded in optimum cutting temperature compound with a thickness of 8 μm were used for Oil Red O staining (catalog no.: O0625; Sigma, St Louis, MO) for fat content observation. After staining, histological images were captured using a light microscope (ECLIPSE 80i; Nikon, Tokyo, Japan) for all staining sections.

### Isolation of primary hepatocytes and in vitro TAK1 inhibitor experiment

Murine primary hepatocytes were isolated from 6- to 8-week-old male mice. After anesthetization, the mice were perfused with liver perfusion medium at 37°C until the liver turned khaki color. The liver was perfused with liver digestion medium containing collagenase IV. After digestion, the livers were removed and the liver capsules were opened to release the hepatocytes into the medium and then filtered through a 70 μm steel mesh. Hepatocytes were obtained by centrifugation at 50 $g$ twice. The cells were grown in DMEM supplemented with 10% fetal bovine serum and 1% penicillin-streptomycin. The cells were maintained in an incubator with 5% $CO_2$. PA and OA stimulation was used to construct a hepatocyte NAFLD model in vitro. For Oil Red O staining, the cells were treated with 0.2 μM PA and 0.4 μM OA for 12 h, and for Western blot and RT-PCR detection, the cells were treated with 0.5 μM PA and 1.0 μM OA for 12 h. For the in vitro iTAK1 experiment, primary hepatocytes were treated with 2 μM iTAK1, 5Z-7-oxozeaenol (catalog no.: O9890-1 MG; Sigma, St. Louis, MO) for 12 h.

### Adenovirus infection

Adenoviruses carrying sequences encoding mouse *Steap3* (Ad.*Steap3*) and hairpin-forming oligonucleotides targeting *Steap3* (Adsh.*Steap3*) were purchased from Hanbio Biotechnology (Shanghai, China). Recombinant adenoviruses were plaque-purified using cesium chloride density gradient centrifugation and verified by restriction digestion. Similar adenoviral vectors that did not carry *the Steap3* gene (Adcontrol) and scrambled short hairpin RNA were used as controls. After purification, the recombinant adenoviruses were diluted to a titer of $10^{10}$ plaque-forming units per milliliter.

### Cellular Nile red staining

Primary hepatocytes on climbing pieces were treated with PA and OA and then fixed with 4% paraformaldehyde for Nile red staining. Primary hepatocytes were stained with 1 μM Nile red (catalog no.: 22190; Fanbo Biochemicals Co, Ltd, Beijing, China) at room temperature for 20 min. The nuclei were stained with 4′,6-diamidino2-phenylindole. Images were obtained using a confocal laser scanning microscope system (TCS SP8; Leica, Wetzlar, Germany).

### RNA extraction and quantitative RT-PCR analysis

Total RNA was extracted from liver tissues or hepatocytes using TRIzol reagent in the phenol-chloroform method and dissolved in diethyl pyrocarbonate-treated water. Subsequently, 1–2 μg of RNA was reverse-transcribed to obtain

cDNA. Quantitative real-time PCR assays were performed with cDNA and specific primers using a real-time PCR system (LightCycler 480 Instrument II) with β-actin as the reference gene. Primer sequences are listed in supplemental Table S1.

## Western blot

Tissues and cells were lysed with radio-immunoprecipitation assay lysis buffer (65 mM Tris-HCl, 150 mM NaCl, 1 mM EDTA, 1% Nonidet P-40, 0.5% sodium deoxycholate, and 1% SDS) supplemented with protease inhibitor. Proteins were separated by high-speed centrifugation and quantified using a bicinchoninic acid protein assay kit. Equivalent amount of protein samples were transferred to PVDF after separating them on 6–10% SDS-PAGE. The membranes were blocked for 1 h at room temperature and sequentially incubated with specific primary antibodies overnight at 4°C, and the corresponding secondary antibodies conjugated with horseradish peroxidase for 1 h at room temperature. The membranes were washed with Tris-buffered saline with Tween-20 three times after blocking and incubation. Finally, chemiluminescence signals were detected and visualized using the ChemiDoc MP Imaging System (Bio-Rad). The antibodies used are listed in supplemental Table S2.

## Coimmunoprecipitation assay

L02 cells transfected with the indicated plasmids were cultivated for 24 h and lysed in cold immunoprecipitation lysis buffer (20 mM Tris-HCl, pH 7.4; 150 mM NaCl; 1 mM EDTA; and 1% Nonidet P-40). After high-speed centrifugation at 4°C, the supernatant containing the protein was incubated with protein G agarose beads and IgG or antitag antibodies at 4°C overnight. Beads were collected by centrifugation at 3,000 rpm at 4°C and washed three times with 150 mM or 300 mM NaCl buffer. Proteins were eluted from the beads with SDS loading buffer and boiled at 95°C for 5–10 min prior to SDS-PAGE and Western blot analysis.

## RNA-Seq and transcriptome analysis

Total RNA extracted from the liver tissue was used for RNA-Seq with MGISEQ 2000 (MGI Tech, China). Differentially expressed genes were identified using two standards: a fold change greater than 2 and the corresponding adjusted $P$ values less than 0.05. The RNA-Seq data have been uploaded to the public database of the National Center for Biotechnology Information (PRJNA900784).

## Hierarchical clustering

Hierarchical clustering creates a hierarchical nested clustering tree by calculating the similarity between different samples, using the weighted average distance (unweighted pair-group method with arithmetic means) algorithm and the HCLUST function of R language for visualization.

## Gene set enrichment analysis

Gene set enrichment analysis (GSEA) uses the gene sets in the Kyoto Encyclopedia of Genes and Genomes (KEGG) pathway to sort genes according to the level of differential expression and subsequently tests whether the gene sets are concentrated at the top or bottom of the sequencing list to obtain the overall expression changes of these gene sets. This analysis was performed on the Java GSEA (version 3.0) platform using the "Signal2Noise" metric, and gene sets with $P$ values less than 0.05 and false discovery rate less than 0.25 were considered statistically significant.

## KEGG pathway enrichment analysis

KEGG is a comprehensive database that integrates genomic, chemical, and systematic functional information. KEGG pathway enrichment analysis was performed for all differentially expressed genes using Fisher's exact test, and KEGG pathway annotations of all genes in the reference genome were downloaded from the KEGG database. Pathways with $P$ values less than 0.05 were defined as significantly enriched pathways.

## Statistical analysis

Data are shown as the mean ± SD. SPSS 21 (IBM Corp., Armonk, NY) was used for the statistical analysis. First, the normality of the data was analyzed. For data conforming to the normal distribution, the two-tailed Student's $t$ test was used for comparative analysis between the two groups, and a one-way ANOVA was used for comparative analysis of three or more groups. Specifically, the Bonferroni test was used for groups with variance homogeneity, and Tamhane's T2 analysis was used for groups with variance heterogeneity. Nonparametric tests were used for data that did not conform to normal distribution. Statistical significance was set at $P < 0.05$.
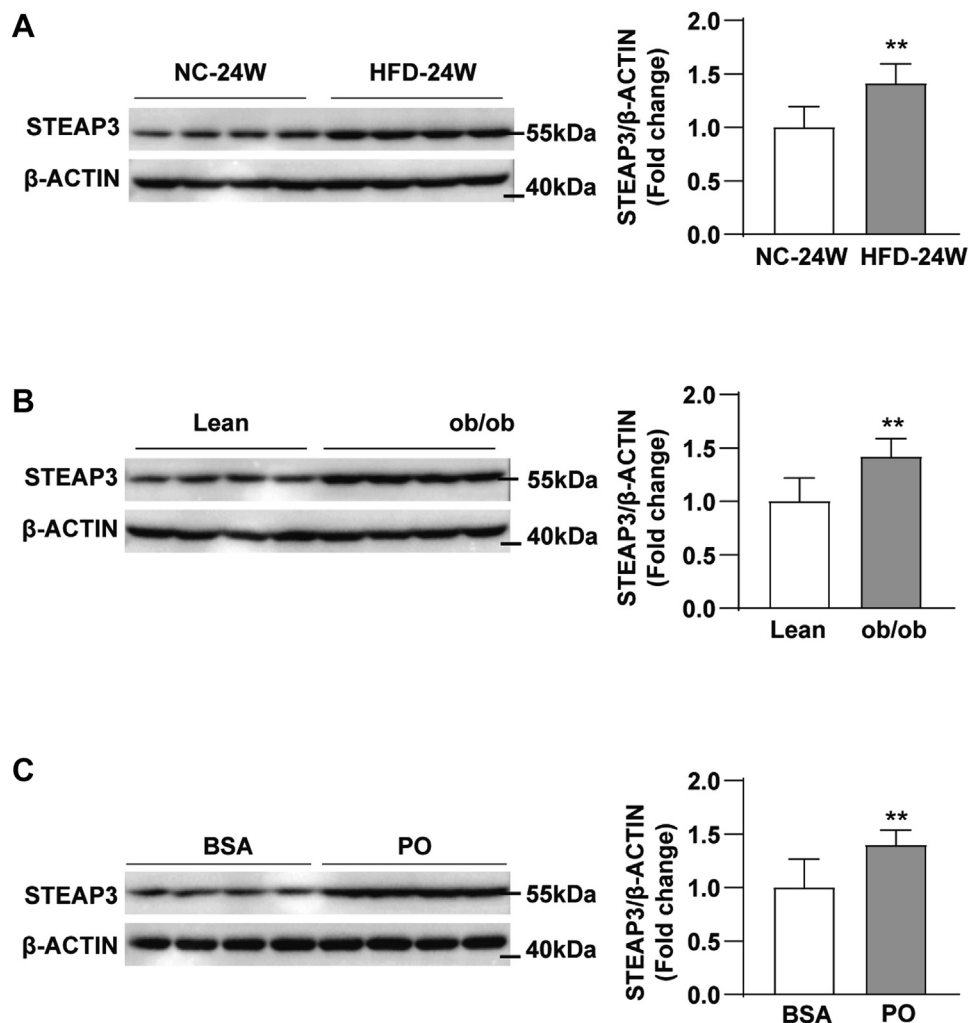
## RESULTS

### STEAP3 is upregulated in NAFLD mice and cell models

To investigate the association between STEAP3 and NAFLD, we determined STEAP3 expression in HFD-induced NAFLD mouse model. Compared with normal controls, STEAP3 levels upregulated significantly in liver tissues of the NAFLD group (Fig. 1A). The same phenomenon was observed in genetically obese (*ob/ob*) mice (Fig. 1B). Consistent with the results in mouse models, STEAP3 levels increased in primary hepatocytes after PA/OA treatment compared with that in cells treated with BSA (Fig. 1C). Taken together, these findings suggest that STEAP3 levels are increased in lipid-laden hepatocytes.

### STEAP3 promotes lipid accumulation in hepatocytes

Given that the expression level of STEAP3 is upregulated in NAFLD, we overexpressed STEAP3 in primary hepatocytes using adenovirus infection to study its effect on NAFLD in vitro. We first confirmed the overexpression of STEAP3 (Fig. 2A). PA/OA stimulation was used to establish cell models, followed by Nile red staining; we found that STEAP3 overexpression promoted PA/OA-induced lipid accumulation in the hepatocytes (Fig. 2B). Consistently, RT-PCR revealed that the mRNA levels of fatty acid synthesis and transport-related genes *Acaca*, *Fads2*, *Fasn*, and *Cd36* were upregulated in STEAP3-overexpressed hepatocytes

**Fig. 1.** STEAP3 is upregulated in NAFLD mice and cell models. A; Representative Western blot analysis and quantitative results of STEAP3 protein expression in liver tissue of NC control or HFD mice. $n = 4$ mice in each group. B: Representative Western blot analysis and quantitative results of STEAP3 protein expression in liver tissue of lean or obese (*ob/ob*) mice. $n = 4$ mice in each group. C: Representative Western blot analysis and quantitative results of STEAP3 protein expression in primary hepatocytes treated with BSA or PA/OA. $n = 4$ independent experiments. Statistical analysis was carried out by two-tailed Student's *t*-test. **$P < 0.01$.

following PA/OA treatment (Fig. 2C). In contrast, when we knockdown STEAP3 in primary hepatocytes by adenovirus infection (Fig. 2D), opposite results were obtained, as evidenced by the reduced lipid accumulation and decreased mRNA levels of lipid metabolism-related genes (Fig. 2E, F). Taken together, our findings suggest that STEAP3 promotes lipid accumulation in the hepatocytes.

### Steap3 deficiency inhibits glucose metabolic disorder induced by HFD

We used *Steap3* systemic gene KO mice to investigate the function of *Steap3* deletion in NAFLD; WT mice were used as controls. An HFD for 24 weeks was used to establish an NAFLD model. We first confirmed the *Steap3* deficiency using Western blot analysis (**Fig. 3**A). NC-fed *Steap3*-KO and WT mice exhibited comparable metabolic characteristics (Fig. 3B–G). However, after 24 weeks of HFD, the fasting body weights, fasting blood glucose levels,

serum insulin content, and homeostatic model assessment of insulin resistance of the KO mice were lower than those of the WT mice (Fig. 3B–E). In addition, the glucose tolerance test assay proved that the loss of *Steap3* significantly enhanced the glucose tolerance induced by the HFD (Fig. 3F, G). To further confirm the abnormality of glucose metabolism, we performed periodic acid-Schiff staining of liver sections and found enhanced glycogen accumulation in KO-HFD mice (Fig. 3H). In line with the results mentioned previously, the RT-PCR assay revealed downregulation of *G6pc* and *Pck1* mRNA levels, indicating that *Steap3* deficiency inhibits gluconeogenesis (Fig. 3I, J). Collectively, Steap3 deletion leads to resistance of diet-induced obesity.

### Steap3 KO relieves HFD-induced hepatic steatosis

Besides glucose metabolic disorder, KO mice showed lower liver weight, liver weight/body weight ratio, serum triglyceride, and total cholesterol contents than
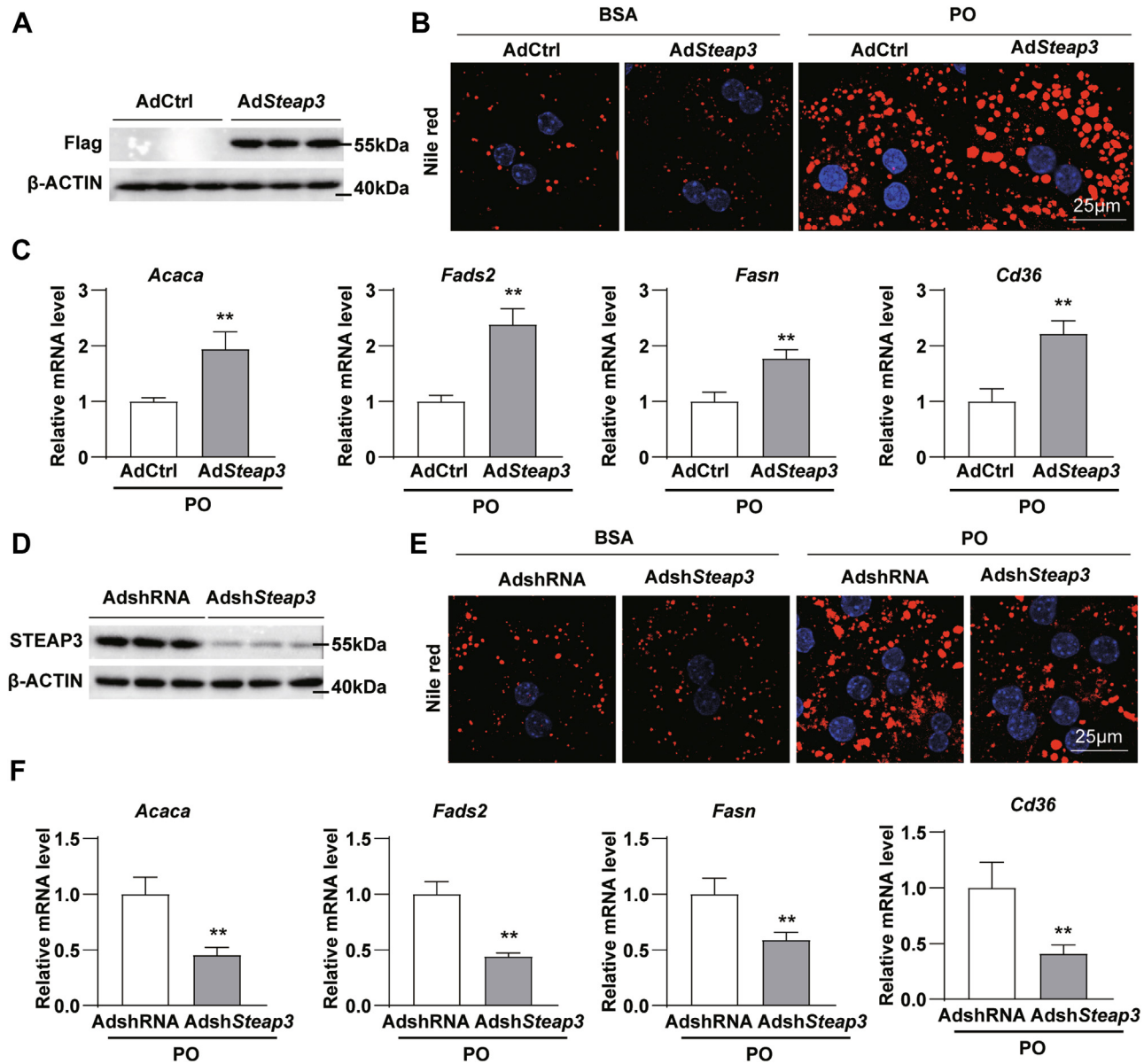
**Fig. 2.** STEAP3 promotes lipid accumulation in hepatocytes. A: Representative Western blot results for STEAP3 overexpression detection in the indicated groups. B: Representative images of Nile red staining of control and STEAP3 overexpression primary hepatocytes treated with BSA or PA/OA. C: Representative RT-PCR analysis results of lipid metabolic genes *Acaca*, *Fads2*, *Fasn*, and *Cd36* in the indicated groups. D: Representative Western blot results for STEAP3 knockdown detection in the indicated groups. E: Representative images of Nile red staining in the indicated groups. F: Representative RT-PCR analysis results of lipid metabolic genes *Acaca*, *Fads2*, *Fasn*, and *Cd36* in the indicated groups. For A, B, D, and E, $n = 3$ independent experiments. For *C* and *F*, $n = 4$ independent experiments. Statistical analysis was carried out by two-tailed Student's *t*-test. **$P < 0.01$.

that of WT mice after HFD, whereas these parameters did not differ clearly during NC feeding (Fig. 4A–D). Similarly, H&E and Oil Red O staining demonstrated reduced hepatic lipid accumulation and steatosis in KO-HFD mice (Fig. 4E, F). Further RT-PCR results revealed that the mRNA levels of fatty acid synthesis and transport-related genes, including *Srebp-1c*, *Acaca*, *Fads2*, *Fasn*, and *Cd36*, decreased significantly, whereas β-oxidation-related gene *Cpt1a* was upregulated (Fig. 4G–L), confirming the effect of *Steap3* deletion in alleviating lipid metabolic disorder. In addition, KO-HFD mice showed lower serum levels of alanine

aminotransferase and aspartate aminotransferase than that of WT-HFD mice (Fig. 4M, N). Collectively, these results revealed that *Steap3* KO mitigated the development of NAFLD.

**STEAP3 significantly regulates glucose metabolism- and lipid metabolism-related pathways**

To profile the differences in gene expression resulting from *Steap3* deletion during NAFLD, the livers of *Steap3*-KO and WT mice after 24 weeks of HFD were subjected to RNA-Seq analysis. Through principal component analysis, the samples from KO and WT
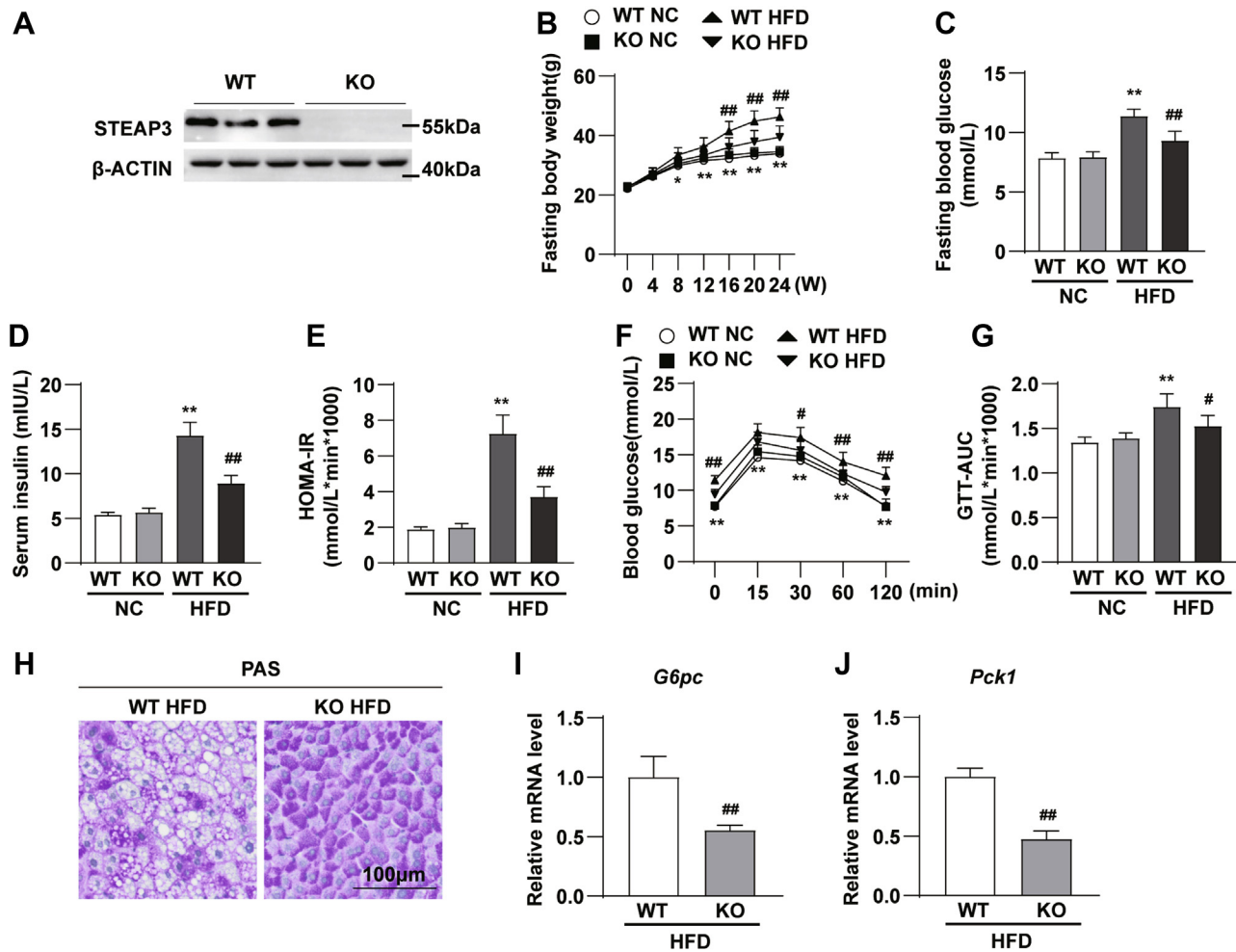
**Fig. 3.** STEAP3 deficiency inhibits glucose metabolic disorder induced by HFD. A: Representative Western blot results of STEAP3 in liver tissue of WT and STEAP3-KO mice. $n = 3$ mice in each group. B–E: Representative fasting body weights (B), fasting blood glucose levels (C), fasting insulin levels (D), and HOMA-IR indices (E) of KO mice and their littermate controls at the indicated time points in response to HFD feeding. $n = 8$–10 mice in each group. F and G: Representative GTT assays and AUC detection results of WT and KO mice fed with NC or HFD for 23 weeks. $n = 8$–10 mice in each group. H: Representative PAS staining images of liver sections in the indicated groups. Bar represents 100 μm, $n = 6$–7 mice in each group. I and J: Representative RT-PCR analysis of glucose metabolic gene *G6pc* and *Pck1* mRNA levels in liver of HFD WT and KO mice. $n = 4$ in each group. B to G: Statistical analysis was carried out by one-way ANOVA. I and J: Statistical analysis was carried out by two-tailed Student's *t*-test. *$P < 0.05$ and **$P < 0.01$ versus WT NC group. #$P < 0.05$ and ##$P < 0.01$ versus WT HFD group. AUC, area under the curve; GTT, glucose tolerance test; HOMA-IR, homeostatic model assessment of insulin resistance; PAS, periodic acid-Schiff.

mice were separated into two clusters based on their gene expression similarities (**Fig. 5**A). GSEA showed that glucose metabolism and lipid metabolism response-related pathways were inactive because of *Steap3* deficiency (Fig. 5B). Heat maps of transcriptome analysis showed decreased activation of lipid metabolism-related (Fig. 5C) and glycometabolism-related (Fig. 5D) genes in the *Steap3*-KO group.

## STEAP3 interacts with TAK1 and activates the TAK1-c-Jun N-terminal kinase/P38 signaling pathway

To further elucidate the underlying mechanism of the effect of STEAP3 on NAFLD, KEGG pathway enrichment analysis was performed, and results showed that the MAPK pathway was the most significantly

enriched signaling pathway (**Fig. 6**A). This indicated that the MAPK signaling pathway might be involved in the function of STEAP3 in NAFLD. To further elucidate the underlying effect of STEAP3 on MAPK pathway activation, we examined the activation of MAPK-related molecules in HFD-induced animal and PA/OA-stimulated cell models. Western blotting results showed that phosphorylation of c-Jun N-terminal kinase (JNK) and p38 in the liver tissues of HFD *Steap3*-KO mice was inhibited, whereas total JNK, p38, ERK1/2, and phosphorylated ERK1/2 remained unchanged (Fig. 6B). Similar changes were observed in primary STEAP3 knockdown hepatocytes stimulated by PA/OA (Fig. 6C). However, STEAP3 overexpression in PA/OA-treated primary hepatocytes exacerbated the phosphorylation of JNK and p38 but not ERK1/2 (Fig. 6D).
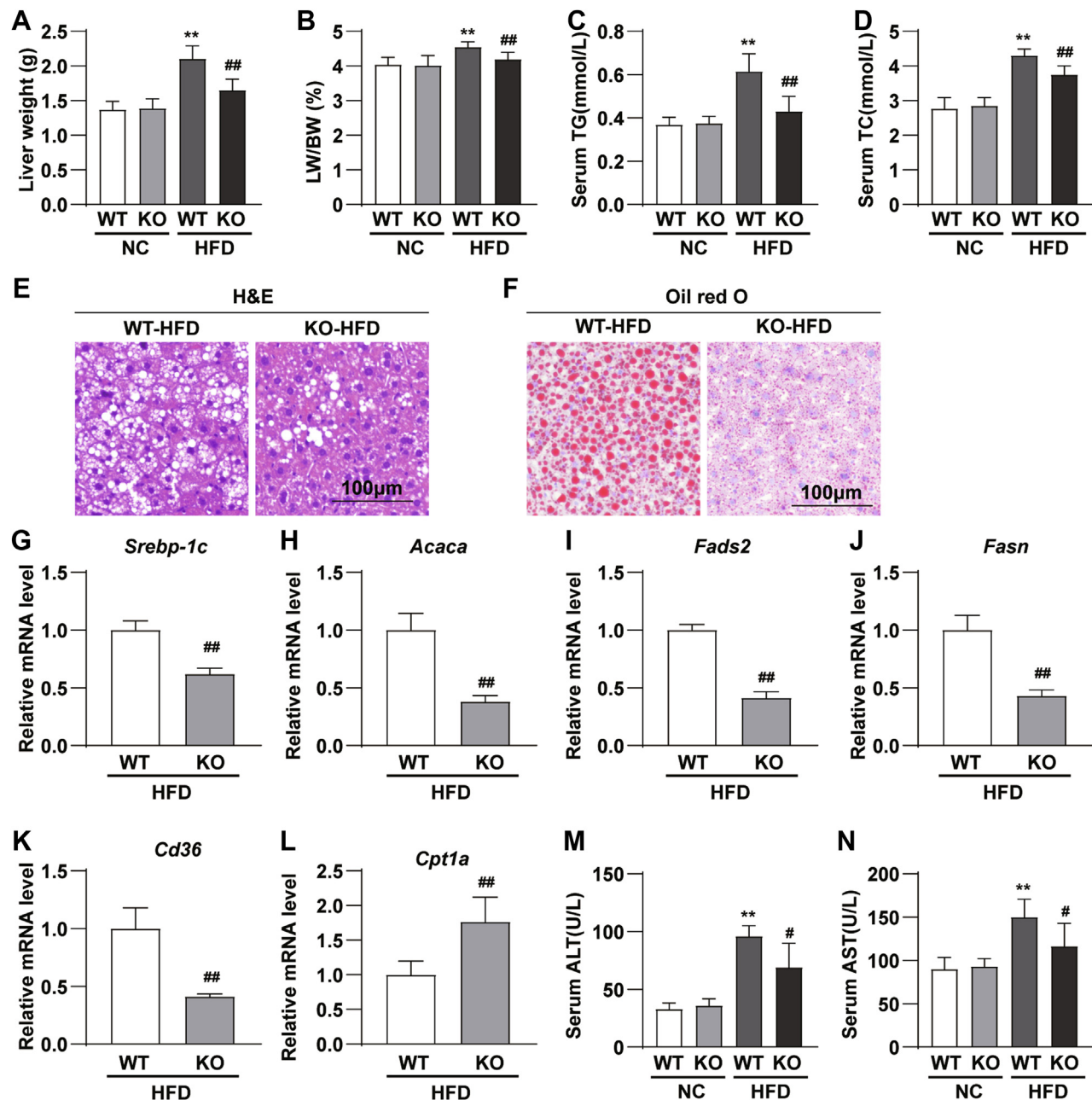
**Fig. 4.** STEAP3 KO relieves HFD-induced hepatic steatosis. A and B: Liver weight (A) and liver weight/body weight ratio (B) of WT and KO mice fed with NC or HFD for 24 weeks. $n = 8$–10 mice in each group. C and D: Serum TG and total cholesterol (TC) levels in WT and KO mice fed with NC or HFD for 24 weeks. $n = 8$–10 mice in each group. E and F: Representative H&E (E) and Oil Red O (F) staining images of liver section from HFD WT and KO mice. Bar represents 100 μm. $n = 6$–7 mice in each group. G–L: Representative RT-PCR analysis of lipid metabolic genes *Srebp-1c*, *Acaca*, *Fads2*, *Fasn*, *Cd36*, and *Cpt1a* mRNA levels in liver of HFD WT and KO mice. $n = 4$ in each group. M and N: Serum alanine aminotransferase (ALT) and aspartate aminotransferase (AST) levels in WT and KO mice fed with NC or HFD for 24 weeks. $n = 8$–10 mice in each group. A to D, M, and N: Statistical analysis was carried out by one-way ANOVA. G to L: Statistical analysis was carried out by two-tailed Student's *t*-test. *$P < 0.05$ and **$P < 0.01$ versus WT NC group. #$P < 0.05$ and ##$P < 0.01$ versus WT HFD group.

As upstream regulatory molecules of MAPK signaling pathway, TAK1 has been reported to be involved in the activation regulation of JNK and p38 (16). Therefore, the levels of total and phosphorylated TAK1 in the above samples were determined, and the results showed that STEAP3 promoted the phosphorylation of TAK1 (Fig. 6E–G). In addition, STEAP3 has been reported to interact with TAK1 during hepatic ischemia-reperfusion injury (15). We overexpressed STEAP3 in primary hepatocytes and showed that STEAP3 interacts with TAK1 under PA/OA stimulation (Fig. 6H). Altogether, our results demonstrate that STEAP3 interacts
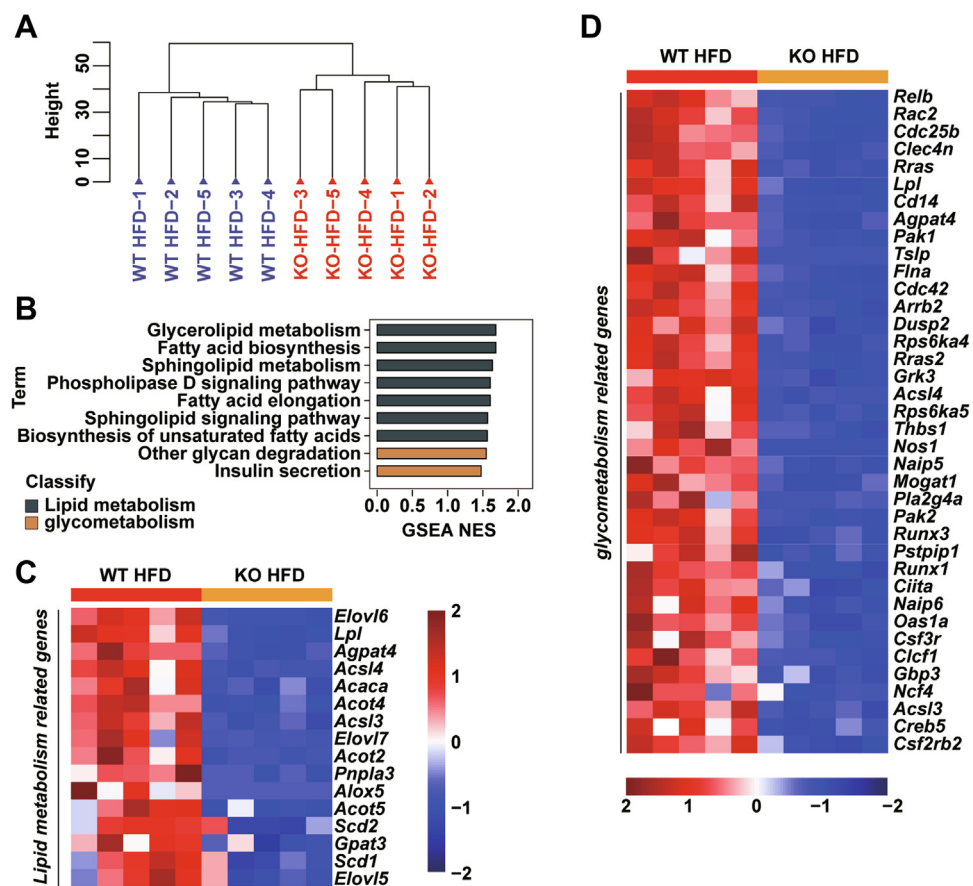
**Fig. 5.** STEAP3 significantly regulates glucose metabolism- and lipid metabolism-related pathways. A: Unsupervised hierarchical clustering analysis of the RNA-Seq data from the mice fed with HFD for 24 weeks B: GSEA pathway enrichment analysis of pathways related to lipid metabolism and glycometabolism. C and D: Heat map of lipid metabolism–related and glycometabolism-related gene expression profiles based on the RNA-Seq dataset. $n = 5$ mice per group.

with TAK1 and regulates the TAK1-JNK/p38 signaling pathway in NAFLD.

### TAK1 inhibition abolishes the regulation of STEAP3 overexpression on lipid accumulation in hepatocytes

To further explore whether STEAP3 regulation of NAFLD depends on TAK1 activation, we used an inhibitor of TAK1 (iTAK1) phosphorylation in PA/OA-stimulated STEAP3 overexpression primary hepatocytes. iTAK1 significantly inhibited the phosphorylation of TAK1, JNK, and p38. And the upregulated phosphorylation of TAK1, JNK, and p38 induced by STEAP3 overexpression was eliminated by iTAK1 (Fig. 7A). Nile red staining showed that, compared with the DMSO-treated control, the accumulation of lipids induced by STEAP3 overexpression was abolished by iTAK1 (Fig. 7B). Moreover, upon iTAK1 treatment, the mRNA level of lipid metabolism-related genes upregulated by STEAP3 overexpression was attenuated significantly, indicating that iTAK1 could reverse lipid metabolism disorder induced by STEAP3 overexpression (Fig. 7C). Collectively, our results suggest

that STEAP3 KO alleviates the development of NAFLD via the TAK1-JNK/p38 signaling pathway.

### DISCUSSION

NAFLD has become the fastest growing liver disease worldwide over the past two decades and is predicted to be the leading cause of end-stage liver disease and liver transplantation (17, 18). NAFLD progression can be followed by the development of fibrosis, liver cirrhosis, liver failure, and HCC (19–21). As a result of lipid metabolism disorders, the presence and accumulation of lipid droplets in over 5% of hepatocytes is known to be the predominant hallmark of NAFLD (22). In the present study, we provide evidence that the absence of STEAP3 inhibits diet-induced NAFLD by improving glucose metabolism disorders and lipid accumulation in hepatocytes. With respect to mechanisms, STEAP3 KO relieves metabolic disorder via interaction with TAK1 to suppressive MAPK signaling pathway.

NAFLD is a liver disease closely related to abnormal glucose and lipid metabolism, and most patients with NAFLD have glucose metabolism disorders (23).
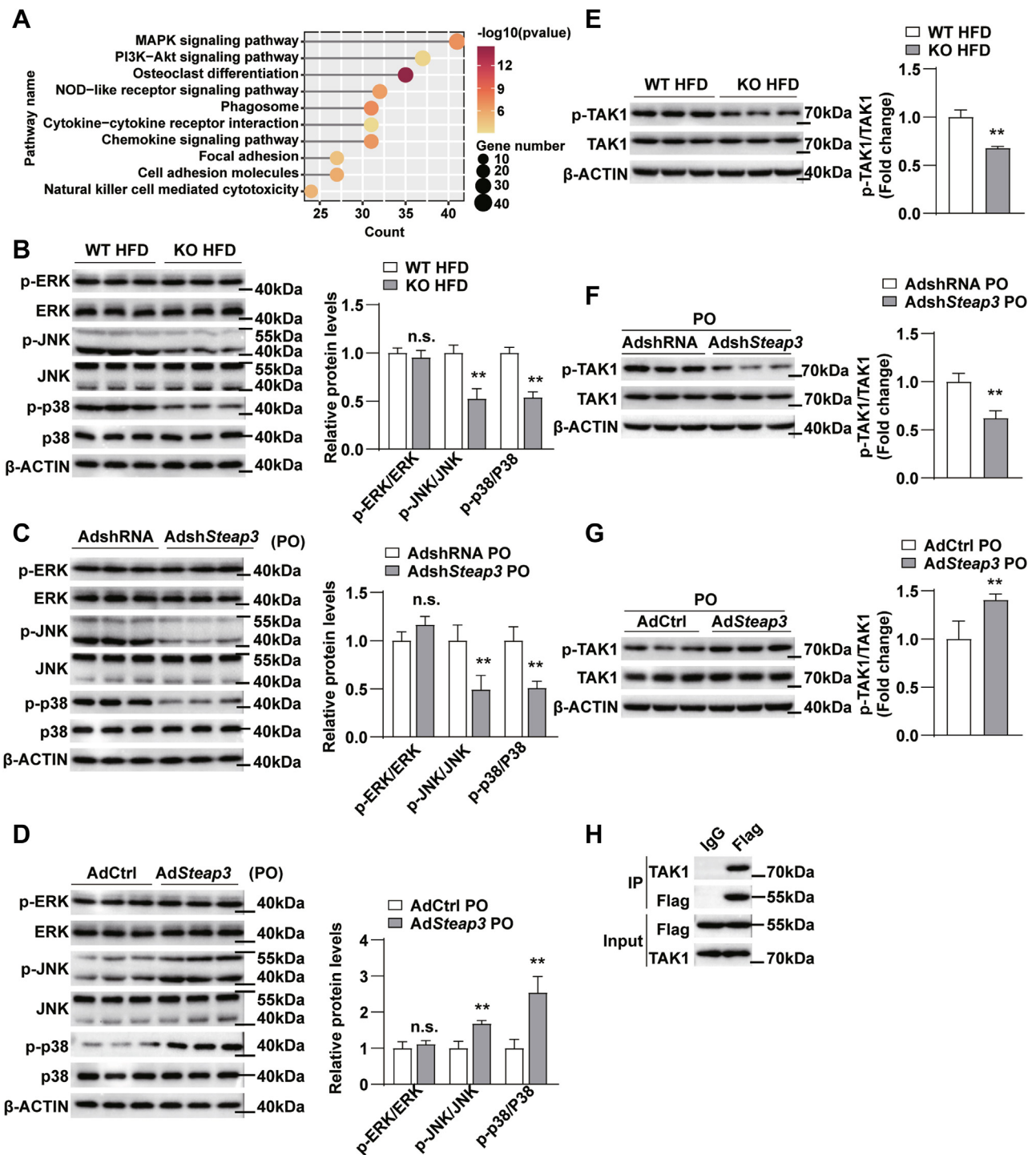
**Fig. 6.** STEAP3 interacts with TAK1 and regulates the TAK1-JNK/P38 signaling pathway. A: KEGG pathway enrichment analysis based on the RNA-Seq dataset. B–D: Representative Western blot analysis of protein levels of total and phosphorylated ERK, JNK, and p38 in liver of WT and KO mice fed with HFD for 24 weeks (B), PA/OA-stimulated STEAP3-KO primary hepatocytes (C), and PA/OA-stimulated STEAP3-overexpressed primary hepatocytes (D). E–G: Representative Western blot analysis of protein levels of total and phosphorylated TAK1 in the indicated groups. H: Representative coimmunoprecipitation analysis of TAK1 and STEAP3 in PA/OA-stimulated hepatocytes. $n = 3$ independent experiments.

Long-term overnutrition can cause insulin resistance in the liver, resulting in glucose metabolism damage (24, 25). In addition, insulin resistance can inhibit the hydrolysis of triglycerides in vivo, increase the decomposition of peripheral adipose tissue, and allow a large number of free fatty acids to enter the liver through the portal vein system, resulting in fatty liver (26–28). Studies have shown that HFD-induced insulin resistance and gluconeogenesis can regulate the progression of NAFLD (29–31). STEAP family proteins are unique to mammals and share innate activities as metalloreductases. In previous studies, STEAP family
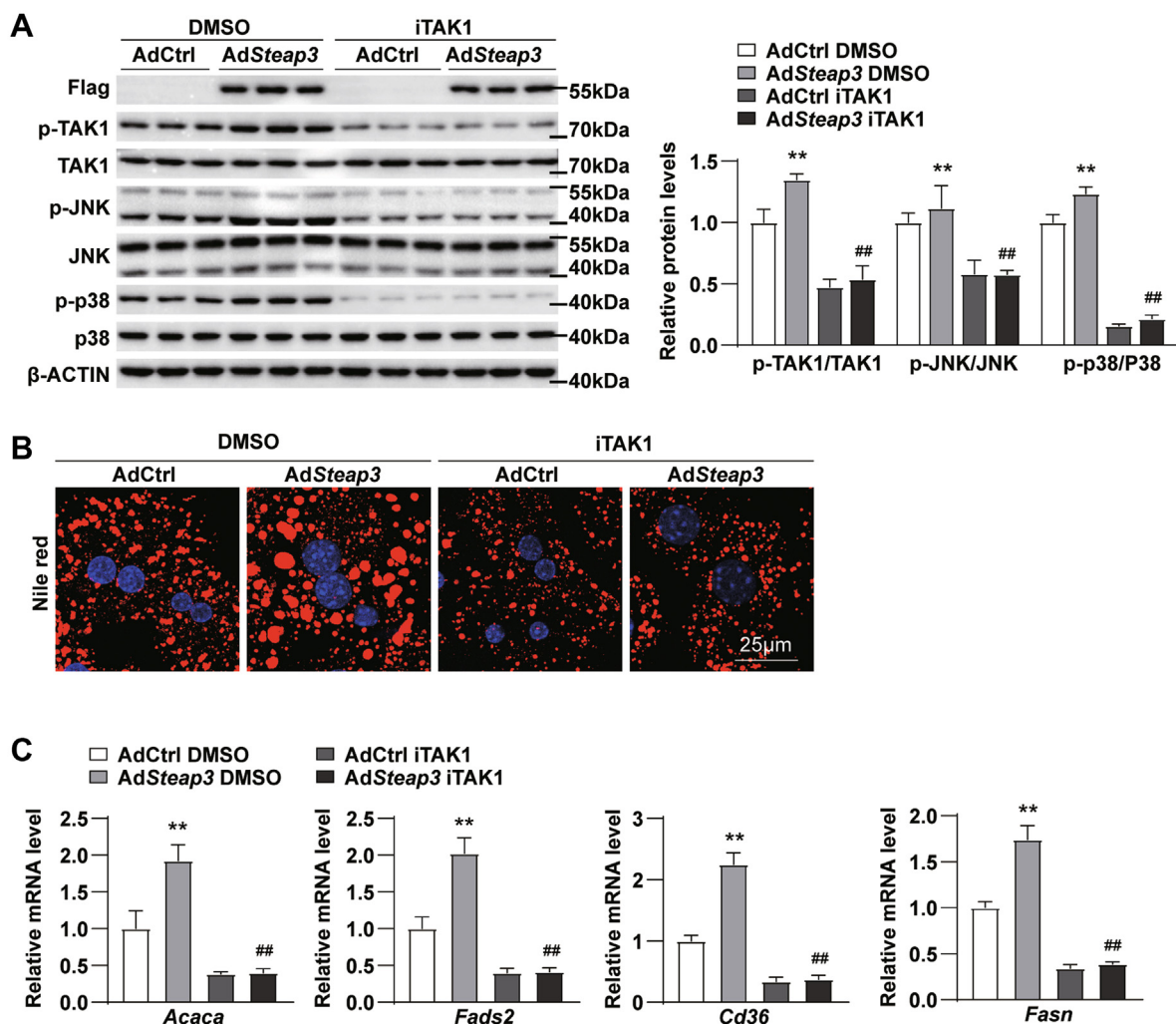
**Fig. 7.** TAK1 inhibition abolishes the regulation of STEAP3 overexpression on lipid accumulation in hepatocytes. A: Representative Western blot analysis of STEAP3, total and phosphorylated TAK1, JNK, and p38 in control and STEAP3 overexpression primary hepatocytes treated with DMSO or iTAK1. $n = 3$ in each group. B: Representative images of Nile red staining of control and STEAP3 overexpression primary hepatocytes treated with DMSO or iTAK1. C: Representative RT-PCR analysis of lipid metabolic genes *Acaca*, *Fads2*, *Cd36*, and *Fasn* in control and STEAP3 overexpression primary hepatocytes treated with DMSO or iTAK1. $n = 4$ independent experiments in each group. Statistical analysis was carried out by one-way ANOVA. $*P < 0.05$ and $**P < 0.01$ versus control DMSO group. $\#P < 0.05$ and $\#\#P < 0.01$ versus STEAP3 DMSO group.

proteins were found to be involved in metabolic diseases, such as insulin resistance and obesity (32–34). For example, STEAP4 promotes insulin-stimulated glucose uptake and regulates insulin sensitivity in mature human adipocytes (33). However, the function of the STEAP family proteins in NAFLD remains unknown. In this study, STEAP3 was found to be involved in the regulation of HFD-induced glucose metabolism and liver lipid deposition, which proved the regulatory role of STEAP family proteins in NAFLD for the first time.

The MAPK signaling pathway has been reported to play a prominent role in the regulation of metabolism in the liver (35). Fatty liver activates stress-responsive MAPKs such as p38 MAPKs and JNKs (36, 37). TAK1, a key upstream regulator of MAPK cascade activation, is a MAPK kinase family serine threonine kinase that plays a critical role in the regulation of autophagy, inflammation, and lipid metabolism (38). TAK1 can hyperactivate downstream JNK and NF-κB signaling, which has been proven to promote the development of steatohepatitis (31). Conversely, degradation of activated phosphorylated TAK1 ameliorates NAFLD in a mouse model (39). However, TAK1 deficiency also leads to severe hepatosteatosis and HCC (40). Because of the dual effect of TAK1 on NAFLD, inhibition of hyperactivation of TAK1 without abolishing its physiological function may be a potential therapeutic treatment for NAFLD (38). Here, we demonstrated for the first time that STEAP3 interacts with TAK1 to regulate the phosphorylation level of TAK1 and thus the progress of NAFLD type C, suggesting that STEAP3 has the potential to be a novel therapeutic target for NAFLD.

This study has some limitations. Systematic, instead of cell type-specific, STEAP3 KO mice were used to construct an in vivo NAFLD model. However, the use of global KO mice in this study increases the difficulty of

determining the effect of STEAP3 on body weight gain after fed HFD for 24 weeks, which needs to be verified in the future with liver-specific KO mice. But, liver-specific KO or overexpression had also been reported to affect body weight in mice induced by HFD treatment ([41], [42]). The hepatocyte-specific effects of STEAP3 KO in pathological NAFLD must be thoroughly elucidated in hepatocyte-specific KO mice.

In conclusion, our study revealed that the interaction between STEAP3 and TAK1 enhances the activation of the MAPK signaling pathway. STEAP3 deficiency protected against diet-induced NAFLD including glucose and lipid accumulation in the liver tissue by inhibiting phosphorylation of TAK1, JNK, and P38. Importantly, these findings may provide new insights into the mechanism of NAFLD and a new approach for the development of an effective treatment of NAFLD by targeting STEAP3.

## Data Availability

The datasets that support the findings of this study are available in this article or the supplemental data.

*Author Contributions*
T. D., S. C., W. X., and W. C. methodology; Y. Y., B. D., and W. C. formal analysis; Z. L., J. T., and W. C. investigation; W. C. writing–original draft; W. C. and Y. Z. supervision; Y. Z. funding acquisition.

*Author ORCIDs*
Wenchang Xiao https://orcid.org/0000-0002-7256-4871

*Abbreviations*
GSEA, gene set enrichment analysis; HCC, hepatocellular carcinoma; HFD, high-fat diet; iTAK1, inhibitor of TAK1; JNK, c-Jun N-terminal kinase; KEGG, Kyoto Encyclopedia of Genes and Genomes; NAFLD, nonalcoholic fatty liver disease; NC, normal chow; PA/OA, palmitic acid/oleic acid; STEAP3, six-transmembrane epithelial antigen of prostate 3; TAK1, transforming growth factor beta-activated kinase 1.

## REFERENCES

1. Lazarus, J. V., Mark, H. E., Villota-Rivas, M., Palayew, A., Carrieri, P., Colombo, M., *et al.* (2022) The global NAFLD policy review and preparedness index: are countries ready to address this silent public health challenge? *J. Hepatol.* **76**, 771–780
2. Younossi, Z., Tacke, F., Arrese, M., Chander Sharma, B., Mostafa, I., Bugianesi, E., *et al.* (2019) Global Perspectives on nonalcoholic fatty liver disease and nonalcoholic steatohepatitis. *Hepatology.* **69**, 2672–2682
3. Hardy, T., Oakley, F., Anstee, Q. M., and Day, C. P. (2016) Nonalcoholic Fatty Liver Disease: pathogenesis and Disease spectrum. *Annu. Rev. Pathol.* **11**, 451–496
4. Foerster, F., Gairing, S. J., Muller, L., and Galle, P. R. (2022) NAFLD-driven HCC: safety and efficacy of current and emerging treatment options. *J. Hepatol.* **76**, 446–457
5. Chen, Z., Yu, Y., Cai, J., and Li, H. (2019) Emerging molecular targets for treatment of nonalcoholic fatty liver disease. *Trends Endocrinol. Metab.* **30**, 903–914
6. Ratziu, V., Francque, S., and Sanyal, A. (2022) Breakthroughs in therapies for NASH and remaining challenges. *J. Hepatol.* **76**, 1263–1278
7. Review, T., LaBrecque, D. R., Abbas, Z., Anania, F., Ferenci, P., Khan, A. G., *et al.* (2014) World Gastroenterology Organisation Global Guidelines: nonalcoholic fatty liver disease and nonalcoholic steatohepatitis. *J. Clin. Gastroenterol.* **48**, 467–473
8. Zhang, H. J., He, J., Pan, L. L., Ma, Z. M., Han, C. K., Chen, C. S., *et al.* (2016) Effects of moderate and vigorous exercise on nonalcoholic fatty liver disease: a randomized clinical trial. *JAMA Intern. Med.* **176**, 1074–1082
9. Chen, W. J., Wu, H. T., Li, C. L., Lin, Y. K., Fang, Z. X., Lin, W. T., *et al.* (2021) Regulatory roles of six-transmembrane epithelial antigen of the prostate family members in the occurrence and development of malignant tumors. *Front. Cell Dev. Biol.* **9**, 752426
10. Gomes, I. M., Maia, C. J., and Santos, C. R. (2012) STEAP proteins: from structure to applications in cancer therapy. *Mol. Cancer Res.* **10**, 573–587
11. Zhang, F., Tao, Y., Zhang, Z., Guo, X., An, P., Shen, Y., *et al.* (2012) Metalloreductase Steap3 coordinates the regulation of iron homeostasis and inflammatory responses. *Haematologica.* **97**, 1826–1835
12. Passer, B. J., Nancy-Portebois, V., Amzallag, N., Prieur, S., Cans, C., Roborel de Climens, A., *et al.* (2003) The p53-inducible TSAP6 gene product regulates apoptosis and the cell cycle and interacts with Nix and the Myt1 kinase. *Proc. Natl. Acad. Sci. U. S. A.* **100**, 2284–2289
13. Blanc, L., Papoin, J., Debnath, G., Vidal, M., Amson, R., Telerman, A., *et al.* (2015) Abnormal erythroid maturation leads to microcytic anemia in the TSAP6/Steap3 null mouse model. *Am. J. Hematol.* **90**, 235–241
14. Lespagnol, A., Duflaut, D., Beekman, C., Blanc, L., Fiucci, G., Marine, J. C., *et al.* (2008) Exosome secretion, including the DNA damage-induced p53-dependent secretory pathway, is severely compromised in TSAP6/Steap3-null mice. *Cell Death Differ.* **15**, 1723–1733
15. Guo, W. Z., Fang, H. B., Cao, S. L., Chen, S. Y., Li, J., Shi, J. H., *et al.* (2020) Six-transmembrane epithelial antigen of the prostate 3 deficiency in hepatocytes protects the liver against ischemia-reperfusion injury by suppressing transforming growth factor-β-activated kinase 1. *Hepatology.* **71**, 1037–1054
16. Wang, J., Ma, J., Nie, H., Zhang, X. J., Zhang, P., She, Z. G., *et al.* (2021) Hepatic regulator of G protein signaling 5 ameliorates nonalcoholic fatty liver disease by suppressing transforming growth factor beta-activated kinase 1-c-Jun-N-terminal kinase/p38 signaling. *Hepatology.* **73**, 104–125
17. Noureddin, M., Vipani, A., Bresee, C., Todo, T., Kim, I. K., Alkhouri, N., *et al.* (2018) NASH leading cause of liver transplant in women: updated analysis of indications for liver transplant and ethnic and gender variances. *Am. J. Gastroenterol.* **113**, 1649–1659
18. Lonardo, A., Nascimbeni, F., Mantovani, A., and Targher, G. (2018) Hypertension, diabetes, atherosclerosis and NASH: cause or consequence? *J. Hepatol.* **68**, 335–352
19. Goldberg, D., Ditah, I. C., Saeian, K., Lalehzari, M., Aronsohn, A., Gorospe, E. C., *et al.* (2017) Changes in the prevalence of Hepatitis C virus infection, nonalcoholic steatohepatitis, and alcoholic liver disease among patients with cirrhosis or liver failure on the waitlist for liver transplantation. *Gastroenterology.* **152**, 1090–1099. e1091
20. Michelotti, G. A., Machado, M. V., and Diehl, A. M. (2013) NAFLD, NASH and liver cancer. *Nat. Rev. Gastroenterol. Hepatol.* **10**, 656–665
21. Villanueva, M. T. (2017) Liver disease: conscious uncoupling in NASH. *Nat. Rev. Drug Discov.* **16**, 238–239
22. European Association for the Study of the, L., European Association for the Study of, D., and European Association for the

Study of, O. (2016) EASL-EASD-EASO Clinical Practice Guidelines for the management of non-alcoholic fatty liver disease. *Diabetologia.* **59**, 1121–1140

23. Bechmann, L. P., Hannivoort, R. A., Gerken, G., Hotamisligil, G. S., Trauner, M., and Canbay, A. (2012) The interaction of hepatic lipid and glucose metabolism in liver diseases. *J. Hepatol.* **56**, 952–964

24. Watt, M. J., Miotto, P. M., De Nardo, W., and Montgomery, M. K. (2019) The liver as an endocrine organ-linking NAFLD and insulin resistance. *Endocr. Rev.* **40**, 1367–1393

25. Bergman, R. N., and Ader, M. (2000) Free fatty acids and pathogenesis of type 2 diabetes mellitus. *Trends Endocrin. Met.* **11**, 351–356

26. Brunt, E. M., Wong, V. W. S., Nobili, V., Day, C. P., Sookoian, S., Maher, J. J., *et al.* (2015) Nonalcoholic fatty liver disease. *Nat. Rev. Dis. Primers.* **1**, 15080

27. Khan, R. S., Bril, F., Cusi, K., and Newsome, P. N. (2019) Modulation of Insulin Resistance in Nonalcoholic Fatty Liver Disease. *Hepatology.* **70**, 711–724

28. Kim, Y. J., Choi, M. S., Woo, J. T., Jeong, M. J., Kim, S. R., and Jung, U. J. (2017) Long-term dietary supplementation with low-dose nobiletin ameliorates hepatic steatosis, insulin resistance, and inflammation without altering fat mass in diet-induced obesity. *Mol. Nutr. Food Res.* **61**. https://doi.org/10.1002/mnfr.201600889

29. Xiang, M., Wang, P. X., Wang, A. B., Zhang, X. J., Zhang, Y. X., Zhang, P., *et al.* (2016) Targeting hepatic TRAF1-ASK1 signaling to improve inflammation, insulin resistance, and hepatic steatosis. *J. Hepatol.* **64**, 1365–1377

30. Wang, P. X., Zhang, X. J., Luo, P. C., Jiang, X., Zhang, P., Guo, J. H., *et al.* (2016) Hepatocyte TRAF3 promotes liver steatosis and systemic insulin resistance through targeting TAK1-dependent signalling. *Nat. Commun.* **7**, 10592

31. Yan, F. J., Zhang, X. J., Wang, W. X., Ji, Y. X., Wang, P. X., Yang, Y., *et al.* (2017) The E3 Ligase Tripartite Motif 8 Targets TAK1 to Promote Insulin Resistance and Steatohepatitis. *Hepatology.* **65**, 1492–1511

32. Arner, P., Stenson, B. M., Dungner, E., Naslund, E., Hoffstedt, J., Ryden, M., *et al.* (2008) Expression of six transmembrane protein of prostate 2 in human adipose tissue associates with adiposity and insulin resistance. *J. Clin. Endocrinol. Metab.* **93**, 2249–2254

33. Chen, X., Zhu, C., Ji, C., Zhao, Y., Zhang, C., Chen, F., *et al.* (2010) STEAP4, a gene associated with insulin sensitivity, is regulated by several adipokines in human adipocytes. *Int. J. Mol. Med.* **25**, 361–367

34. Qin, D. N., Kou, C. Z., Ni, Y. H., Zhang, C. M., Zhu, J. G., Zhu, C., *et al.* (2010) Monoclonal antibody to the six-transmembrane epithelial antigen of prostate 4 promotes apoptosis and inhibits proliferation and glucose uptake in human adipocytes. *Int. J. Mol. Med.* **26**, 803–811

35. Zhang, P., Wang, P. X., Zhao, L. P., Zhang, X., Ji, Y. X., Zhang, X. J., *et al.* (2018) The deubiquitinating enzyme TNFAIP3 mediates inactivation of hepatic ASK1 and ameliorates nonalcoholic steatohepatitis. *Nat. Med.* **24**, 84

36. Olefsky, J. M., and Glass, C. K. (2010) Macrophages, inflammation, and insulin resistance. *Annu. Rev. Physiol.* **72**, 219–246

37. Samuel, V. T., and Shulman, G. I. (2018) Nonalcoholic fatty liver disease as a nexus of metabolic and Hepatic diseases. *Cell Metab.* **27**, 22–41

38. Liu, D., Zhang, P., Zhou, J. J., Liao, R. F., Che, Y., Gao, M. M., *et al.* (2020) TNFAIP3 Interacting Protein 3 Overexpression Suppresses Nonalcoholic Steatohepatitis by Blocking TAK1 Activation. *Cell Metab.* **31**, 726

39. Wang, L., Zhang, X., Lin, Z. B., Yang, P. J., Xu, H., Duan, J. L., *et al.* (2021) Tripartite motif 16 ameliorates nonalcoholic steatohepatitis by promoting the degradation of phospho-TAK1. *Cell Metab.* **33**, 1372–1388.e1377

40. Inokuchi-Shimizu, S., Park, E. J., Roh, Y. S., Yang, L., Zhang, B., Song, J., *et al.* (2014) TAK1-mediated autophagy and fatty acid oxidation prevent hepatosteatosis and tumorigenesis. *J. Clin. Invest.* **124**, 3566–3578

41. Sun, P., Zeng, Q., Cheng, D., Zhang, K., Zheng, J., Liu, Y., *et al.* (2018) Caspase recruitment domain protein 6 protects against hepatic steatosis and insulin resistance by suppressing apoptosis signal-regulating kinase 1. *Hepatology.* **68**, 2212–2229

42. Luo, P., Wang, P. X., Li, Z. Z., Zhang, X. J., Jiang, X., Gong, J., *et al.* (2016) Hepatic Oncostatin M Receptor beta Regulates Obesity-Induced Steatosis and Insulin Resistance. *Am. J. Pathol.* **186**, 1278–1292

ASBMB